


 Cite this: *Metallomics*, 2020, 12, 470

 Received 7th December 2019,
 Accepted 18th February 2020

DOI: 10.1039/c9mt00299e

rsc.li/metallomics

N-Truncated $A\beta_{4-42}$ displays a high binding affinity with Cu^{II} . A mechanistic scheme of the interactions between $A\beta_{4-42}$ and Cu^{II} has been proposed using a fluorescence approach. The timescales of different conversion steps were determined. This kinetic mechanism indicates the potential synaptic functions of $A\beta_{4-42}$ during neurotransmission.

The amyloid- β ($A\beta$) peptides associated with Alzheimer's Disease (AD) comprise a number of species. The "canonical" $A\beta_{1-42}$ and $A\beta_{1-40}$ peptides derived directly by proteolysis of the Amyloid Precursor Protein (APP) are complemented by N- and C-truncated species, yielded by a variety of brain proteases.¹ Among them, the N-truncated $A\beta_{4-42}$ has been reported as particularly abundant in the hippocampus and cortex of sporadic AD patients, as well as in healthy controls,^{2,3} even exceeding $A\beta_{1-42}$ and $A\beta_{1-40}$.^{4,5} $A\beta_{1-x}$ peptides can bind Cu^{II} using the N-terminus and H6, H13, and His14 residues.⁶⁻⁸ Hence, $A\beta_{1-16}$ has been adopted as a common model peptide in metal binding studies. K_d in the range of 0.1 nM to 1 nM at pH 7.1–7.4 was determined for $A\beta_{1-16}$ and $A\beta_{1-40}$.⁹⁻¹¹ The adventitious binding of Cu^{II} ions to $A\beta_{1-42/40}$ and the concomitant generation of reactive oxygen species (ROS) *via* the Cu^{II}/Cu^I redox pair has been proposed to be the molecular basis of oxidative stress and neuronal death in AD.¹² On the other hand, $A\beta_{4-x}$ peptides bind a Cu^{II} ion more than three orders of magnitude more strongly ($K_d = 30$ fM and 6.6 fM at pH 7.4 for $A\beta_{4-16}$ and $A\beta_{4-9}$, respectively), using their N-terminal ATCUN motif spanning the Phe4, Arg5 and His6 residues. These complexes are redox-inert and do not generate significant ROS. Cu^{II} ion transfer from $A\beta_{1-16}$ to $A\beta_{4-16}$ occurs upon adding the latter to the $Cu^{II}A\beta_{1-16}$ solution.¹³

Hierarchical binding of copper^{II} to N-truncated $A\beta_{4-16}$ peptide[†]

 Xiangyu Teng,[‡] Ewelina Stefaniak,[‡] Paul Girvan,[‡] Radostaw Kotuniak,[‡] Dawid Płonka,[‡] Wojciech Bal,[‡] and Liming Ying[‡]

Significance to metallomics

N-Truncated $A\beta_{4-x}$ is abundant in both healthy and AD brains. Its $Cu(II)$ binding affinity is three orders of magnitude stronger than well-known $A\beta_{1-42}$ or $A\beta_{1-40}$. Using a model peptide, $A\beta_{4-16}$, we have elucidated the reaction mechanism of $Cu(II)$ with $A\beta_{4-x}$, crucial to understand the physiological role and toxicity of $A\beta$ peptides. The presence of two kinetic intermediates prior to the formation of the tight ATCUN complex has implications for the potential function of $A\beta_{4-42}$ as a $Cu(II)$ transporter during neurotransmission. The methodology used in this work may also stimulate the research of $Cu(II)$ interactions with other intrinsically disordered proteins (IDPs).

This reaction is quantitative, in agreement with the affinity difference, and fast, occurring within the sample preparation time \sim s. Such a reaction suggested that $A\beta_{4-42}$ should prevail as a Cu^{II} binding $A\beta$ species in the extracellular spaces of the brain. This finding gave rise to a hypothesis that $A\beta_{4-42}$ may have a physiological role as a synaptic Cu^{II} scavenger during neurotransmission.¹⁴ However, Cu^{II} release events in glutamatergic synapses may occur on a much faster, millisecond scale. Therefore, a thorough determination of association and dissociation rate constants for the participating species is necessary to help evaluate their relevance *in vivo*. Such data have been obtained previously for $Cu^{II}A\beta_{1-x}$ complexes.¹⁵⁻¹⁷ Here, we studied the reaction mechanism for Cu^{II} binding to the model peptide $A\beta_{4-16}$ and found that the reaction follows a hierarchical fashion, going through two intermediate states and then reaching the final tight complex.

First, we studied the effect of N-truncation on the Cu^{II} binding kinetics. 20 nM $A\beta$ labelled by HiLyte Fluor 488 on lysine 16 (FRHDSGYEVHHQK-HiLyte 488) was reacted with 400 nM Cu^{II} under various HEPES concentrations in order to obtain the HEPES-independent Cu^{II} binding rate constant (k_{on}). The results are shown in Fig. 1a. The intercept of the fitted curve (Fig. 1b) was used to determine k_{on} , which is $2.0(1) \times 10^8$ $M^{-1} s^{-1}$, 2.5 times slower than the value for $A\beta_{1-16}$.¹⁷

k_{off} was determined for the reaction of a Cu^{II} complex of unlabelled $A\beta_{4-16}$ with an excess of EDTA. The estimated value

^a Department of Chemistry, Imperial College London, Molecular Sciences Research Hub, White City Campus, London W12 0BZ, UK

^b Institute of Biochemistry and Biophysics, Polish Academy of Sciences, Pawińskiego 5a, 02-106 Warsaw, Poland. E-mail: wbal@ibb.waw.pl

^c National Heart and Lung Institute, Imperial College London, Molecular Sciences Research Hub, White City Campus, London W12 0BZ, UK. E-mail: Lying@imperial.ac.uk

[†] Electronic supplementary information (ESI) available. See DOI: 10.1039/c9mt00299e

[‡] These authors contributed equally to this work.

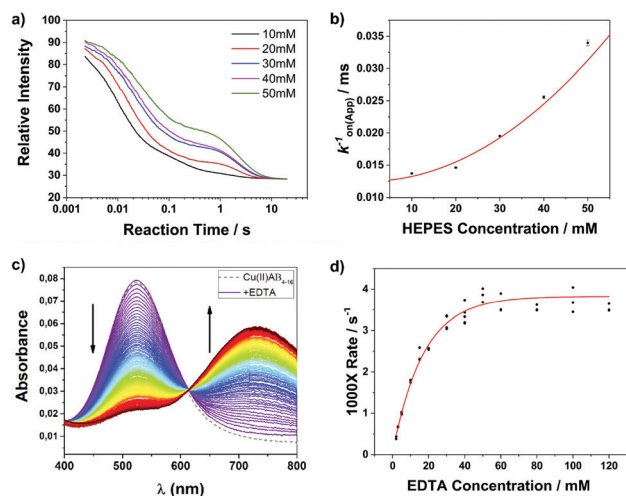



Fig. 1 Kinetics of Cu^{II} binding to $\text{A}\beta_{4-16}$. (a) Representative raw traces of $\text{A}\beta$ (20 nM) with Cu^{II} (400 nM) under various concentrations of HEPES. The experiments were performed in 50 mM HEPES and 100 mM NaCl buffer solution at 298 K (pH 7.5). (b) HEPES dependence of k_{on} . The HEPES independent k_{on} value is $2.0(1) \times 10^8 \text{ M}^{-1} \text{ s}^{-1}$. (c) Kinetics of dissociation of $\text{Cu}^{\text{II}}\text{A}\beta_{4-16}$ assisted by varying concentrations of EDTA, monitored by UV-vis absorbance. The experiments were performed for 1 mM $\text{Cu}^{\text{II}}\text{A}\beta_{4-16}$ at 298 K (pH 7.5). (d) Empirical fit to derive the EDTA-independent k_{off} .

is $\sim 5 \times 10^{-5} \text{ s}^{-1}$, which divided by k_{on} proposed here gives $K_{\text{d}} \sim 250 \text{ fM}$. EDTA is a stronger Cu^{II} chelator than $\text{A}\beta_{4-16}$, with a $\log \beta$ of 18.7, which can be recalculated into a conditional constant ${}^{\text{C}}K$ of 16.0 at pH 7.5.¹⁸ This value is sufficiently higher than that of $\text{Cu}^{\text{II}}\text{A}\beta_{4-16}$, 13.53, to assure full Cu^{II} transfer, as demonstrated in Fig. 1c. The reaction was carried out for a range of EDTA/peptide ratios between 2 and 120. Pseudo-1st order kinetics for the Cu^{II} transfer reaction was observed for all experiments. The non-linear response of k_{off} to EDTA required the EDTA-independent k_{off} value to be determined by the extrapolation of the empirical exponential fit to these data, as shown in Fig. 1d.

To gain a glimpse of a possible reaction mechanism of Cu^{II} binding to N-truncated $\text{A}\beta_{4-16}$, we performed binding experiments at a 1:1 mixing ratio of $\text{A}\beta$ to Cu^{II} with increasing concentration. In such experiments, the effect of the second Cu^{II} binding can be ignored, as the relevant $\log K$ is as low as 6.7.¹³ The raw traces are shown in Fig. 2a. We noticed that the reaction process is becoming concentration independent after $\sim 2 \text{ s}$ (results from the fit are summarized in Table S1, ESI†). Thus we infer the existence of an intramolecular process following the initial Cu^{II} binding.

Next, a double mixing stopped flow technique was employed to further explore the potential intermediate complexes formed after the initial Cu^{II} binding. This technique was successfully applied to probe the interconversion between component I and component II Cu^{II} coordination species of $\text{A}\beta_{1-16}$ and $\text{A}\beta_{1-40}$.¹⁷ $2 \mu\text{M}$ $\text{A}\beta_{4-16}$ and $2 \mu\text{M}$ Cu^{II} were mixed in a delay loop and after various delay times the reaction was “frozen” by adding an excess of EDTA (Fig. 2b). Taking advantage of the disparities in reactivity of different $\text{Cu}^{\text{II}}\text{A}\beta_{4-16}$ species with EDTA, the time evolution of the population of individual species could be

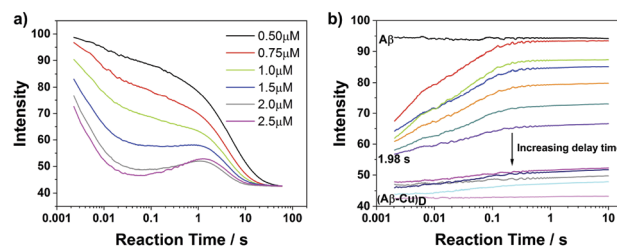


Fig. 2 (a) Raw traces of Cu^{II} binding measurements with a series of 1:1 concentration ratio HiLyte 488 labelled $\text{A}\beta$ and Cu^{II} showing the evidence of intermediate species formation. The experiment was performed in 50 mM HEPES and 100 mM NaCl buffer solution at 298 K (pH 7.5). (b) Kinetics of HiLyte 488 labelled $\text{A}\beta/\text{Cu}^{\text{II}}$ interactions measured by double mixing stopped flow. Raw traces showing the change in amplitude as the delay time between mixing of an equal concentration of Cu^{II} and $\text{A}\beta$ (2 μM) and addition of EDTA is increased from 50 ms to 1 min. The experiment was performed in 50 mM HEPES and 100 mM NaCl buffer solution at 298 K (pH 7.5).

resolved and analyzed, enabling us to depict details of the binding process.

As shown in Fig. 2b, the amplitude of fluorescence recovery strongly depends on the delay time, indicating that a much more inert (less reactive towards EDTA) complex (“dark” complex) formed after around 2 s. We equate this end complex, $(\text{A}\beta\text{-Cu})_{\text{D}}$, to the very stable ATCUN-type $\text{Cu}^{\text{II}}\text{A}\beta_{4-16}$ complex reported previously.¹³ Furthermore, because the reaction rate is concentration independent after 2 s as mentioned above, we propose that a peptide conformational rearrangement process leading to this final complex must occur at around 2 s.

In order to describe the whole process of Cu^{II} binding of N-truncated $\text{A}\beta_{4-16}$, we hypothesized a reaction scheme as shown in Fig. 3a. The individual amplitudes of the two phases in Fig. 2b were determined by a global fit, which were further fitted by the scheme with KinTek software to validate it (Fig. 3b). The amplitudes indicate the amounts of two intermediates, Species I and Species II, at different reaction process stages, and could be

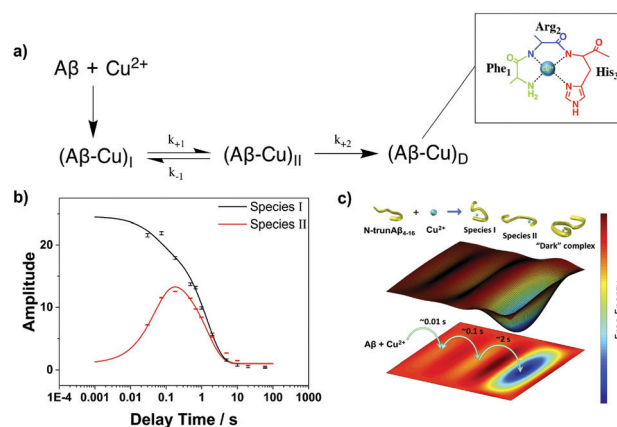


Fig. 3 (a) Reaction mechanism of Cu^{II} binding to $\text{A}\beta_{4-16}$ and formation of the high affinity $\text{Cu}^{\text{II}}\text{A}\beta_{4-16}$ complex, $(\text{A}\beta\text{-Cu})_{\text{D}}$ (Cu^{II} binding site shown above). (b) Fitting of the individual amplitudes at different Cu^{II} binding process stages by the predicted reaction mechanism. (c) Proposed free energy landscape of Cu^{II} binding to $\text{A}\beta_{4-16}$. “Dark” complex refers to the very stable ATCUN-type $\text{Cu}^{\text{II}}\text{A}\beta_{4-16}$ complex.



Table 1 Rate constants corresponding to the mechanism scheme shown in Fig. 3a

	k_{+1}	k_{-1}	k_{+2}
k value/s ⁻¹	4.10(1)	10.34(2)	3.31(4)

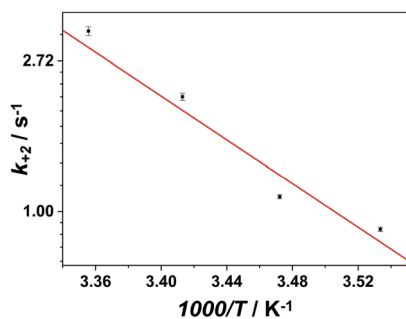


Fig. 4 Arrhenius plot for the switching rate constant k_{+2} . The switching activation energy determined is 64(3) kJ mol⁻¹.

fitted well by the predicted mechanism, with fitted rate constants listed in Table 1. A corresponding free energy landscape illustration of Cu^{II} binding with A β ₄₋₁₆ is shown in Fig. 3c.

Finally, the activation energy of the (A β -Cu)_D complex was determined to be 64(3) kJ mol⁻¹ (Fig. 4) by performing a series of double mixing experiments at different temperatures (raw data shown in Fig. S1, ESI[†]).

The chemical properties of ATCUN Cu^{II} complexes of A β _{4-x} peptides, such as high thermodynamic stability, absence of ROS production due to their resistance to oxidation and reduction, reluctance of copper to transfer to metallothionein-3 (MT3) and easy sequestering of Cu^{II} from A β _{1-x}, gave rise to a concept that A β _{4-x} peptides (full-length A β ₄₋₄₂ and its C-truncated analogs) may serve as guardians of synaptic function, by sequestering excess Cu^{II} ions released during neurotransmission in glutamatergic pathways.^{14,19} The key unsolved issue is how these exchange-inert complexes relay copper back to neurons to maintain the proper copper cycling. Furthermore, Cu^{II}-free A β ₄₋₄₂ can be neurotoxic by forming oligomeric species.²⁰ Detailed knowledge on mechanisms of Cu^{II} association with and dissociation from A β _{4-x} peptides, represented here by A β ₄₋₁₆, is thus crucial to understand the physiology and toxicity of these A β peptides.

The discovery of long-lived kinetic intermediates in the formation of the ATCUN complex of A β ₄₋₁₆ is a game changer in the above considerations. The lifetimes of Species I and Species II complexes are comparable to the intervals between pulses of neurotransmitter release in glutamatergic neuronal pathways.²¹ Therefore, these complexes may well contribute to the biological activity of A β ₄₋₄₂, and of putative short peptidic fragments generated by neprilysin cleavage, such as A β ₄₋₉.^{22,23} There is only one way in which four nitrogen ligands of the ATCUN motif can be arranged around the Cu^{II} ion, and so it is reasonable to assume that the intermediate species contain the coordinatively unsaturated Cu^{II}. Such species have been implicated in the reverse reaction of Cu^{II} dissociative transfer from Cu^{II}A β ₄₋₁₆ to MT3, to explain the catalytic effect of glutamate,²⁴

but it has not been observed directly. The Species I and in particular the longer-lived Species II complex may be the actual species able to move copper around during neurotransmission. The fact that the Cu^{II}A β _{1-x} complex, although so much weaker, was formed 2.5 times faster, prompts further research into possible synaptic roles of Cu^{II} interactions with various A β species.

Furthermore, the observed hierarchical binding of Cu^{II} to A β ₄₋₁₆ resembles the kinetics of the binding of many intrinsically disordered proteins (IDPs).²⁵ The methodology used in this study may be applicable to the fundamental understanding of the emerging “coupled binding and folding” paradigm.²⁶

Conflicts of interest

There are no conflicts to declare.

Acknowledgements

This work was supported by the Leverhulme Trust grant RPG-2015-345 to LY and the Biotechnology and Biosciences Research Council (UK) grant BB/R022429/1 to LY, and the National Science Centre in Poland: PRELUDIUM Grant No. 2016/21/N/NZ1/02785 and ETIUDA Grant No. 2018/28/T/NZ1/00452, to ES, and OPUS Grant No. 2018/29/B/ST4/01634 to WB. The equipment used was sponsored in part by the Centre for Preclinical Research and Technology (CePT) under award number POIG.02.02.00-14-024/08-00, a project co-sponsored by European Regional Development Fund and Innovative Economy, the National Cohesion Strategy of Poland.

Notes and references

- 1 D. J. Selkoe, *Physiol. Rev.*, 2001, **81**, 741–766.
- 2 C. L. Masters, G. Simms, N. A. Weinman, G. Multhaup, B. L. McDonald and K. Beyreuther, *Proc. Natl. Acad. Sci. U. S. A.*, 1985, **82**, 4245–4249.
- 3 E. Portelius, N. Bogdanovic, M. K. Gustavsson, I. Volkman, G. Brinkmalm, H. Zetterberg, B. Winblad and K. Blennow, *Acta Neuropathol.*, 2010, **120**, 185–193.
- 4 G. Antonios, N. Saiepour, Y. Bouter, B. C. Richard, A. Paetau, A. Verkoniemi-Ahola, L. Lannfelt, M. Ingelsson, G. G. Kovacs, T. Pillot, O. Wirths and T. A. Bayer, *Acta Neuropathol. Commun.*, 2013, **1**, 56.
- 5 T. A. Bayer and O. Wirths, *Acta Neuropathol.*, 2014, **127**, 787–801.
- 6 P. Dorlet, S. Gambarelli, P. Faller and C. Hureau, *Angew. Chem.*, 2009, **121**, 9437–9440 (*Angew. Chem., Int. Ed.*, 2009, **48**, 9273–9276).
- 7 B. Alies, H. Eury, C. Bijani, L. Rechinat, P. Faller and C. Hureau, *Inorg. Chem.*, 2011, **50**, 11192–11201.
- 8 E. Atrián-Blasco, P. Gonzalez, A. Santoro, B. Alies, P. Faller and C. Hureau, *Coord. Chem. Rev.*, 2018, **375**, 38–55.
- 9 B. Alies, E. Renaglia, M. Rózga, W. Bal, P. Faller and C. Hureau, *Anal. Chem.*, 2013, **85**, 1501–1508.
- 10 T. R. Young, A. Kirchner, A. G. Wedd and Z. Xiao, *Metalloomics*, 2014, **6**, 505–517.



- 11 A. Conte-Daban, V. Borghesani, S. Sayen, E. Guillon, Y. Journaux, G. Gontard, L. Lisnard and C. Hureau, *Anal. Chem.*, 2017, **89**, 2155–2162.
- 12 C. Cheignon, M. Jones, E. Atrián-Blasco, I. Kieffer, P. Faller, F. Collin and C. Hureau, *Chem. Sci.*, 2017, **8**, 5107–5118.
- 13 M. Mital, N. E. Wezynfeld, T. Frączyk, M. Z. Wiloch, U. E. Wawrzyniak, A. Bonna, C. Tumpach, K. J. Barnham, C. L. Haigh, W. Bal and S. C. Drew, *Angew. Chem.*, 2015, **127**, 10606–10610 (*Angew. Chem., Int. Ed.*, 2015, **54**, 10460–10464).
- 14 E. Stefaniak and W. Bal, *Inorg. Chem.*, 2019, **58**, 13561–13577.
- 15 P. Girvan, T. Miyake, X. Teng, T. Branch and L. Ying, *ChemBioChem*, 2016, **17**, 1732–1737.
- 16 T. Branch, M. Barahona, C. A. Dodson and L. Ying, *ACS Chem. Neurosci.*, 2017, **8**, 1970–1979.
- 17 T. Branch, P. Girvan, M. Barahona and L. Ying, *Angew. Chem.*, 2015, **127**, 1243–1246 (*Angew. Chem., Int. Ed.*, 2015, **54**, 1227–1230).
- 18 J. Felcman and J. J. da Silva, *Talanta*, 1983, **30**, 565–570.
- 19 N. E. Wezynfeld, E. Stefaniak, K. Stachucy, A. Drozd, D. Płonka, S. C. Drew, A. Krężel and W. Bal, *Angew. Chem.*, 2016, **128**, 8375–8378 (*Angew. Chem., Int. Ed.*, 2016, **55**, 8235–8238).
- 20 J. Dunys, A. Valverde and F. Checler, *J. Biol. Chem.*, 2018, **293**, 15419–15428.
- 21 W. Goch and W. Bal, *PLoS One*, 2017, **12**, e0170749.
- 22 M. Mital, W. Bal, T. Frączyk and S. C. Drew, *Inorg. Chem.*, 2018, **57**, 6193–6197.
- 23 K. Bossak-Ahmad, M. Mital, D. Płonka, S. C. Drew and W. Bal, *Inorg. Chem.*, 2019, **58**, 932–943.
- 24 A. Santoro, N. Wezynfeld, E. Stefaniak, A. Pomorski, D. Płonka, A. Krężel, W. Bal and P. Faller, *Chem. Commun.*, 2018, **54**, 12634–12637.
- 25 K. Sugase, H. J. Dyson and P. E. Wright, *Nature*, 2007, **447**, 1021–1025.
- 26 S. Gianni, J. Dogan and P. Jemth, *Curr. Opin. Struct. Biol.*, 2016, **36**, 18–24.

